33rd Annual International Conference of the IEEE EMBS
Boston, Massachusetts USA, August 30 - September 3, 2011

Using Microelectrode Models for Real Time Cell-Culture Monitoring

Alberto Yúfera[1] *Member, IEEE*, Paula Daza[2], Daniel Cañete[3]

***Abstract*: This paper proposes a cell-microelectrode model for cell biometry applications, based on the area overlap as main parameter. The model can be applied to cell size identification, cell count, and their extension to cell growth and dosimetry protocols. Experiments performed with comercial electrodes are presented, illustrating a procedure to obtain cell number in both growth and dosimetry processes. Results obtained for the AA8 cell line are promising.**

Keywords- Microelectrode; ECIS; bio-impedance; impedance sensor; cell culture; dosimetry.

I. INTRODUCTION

Many biological parameters and processes can be sensed and monitored using its impedance as marker [1-5], with the advantage of being a non-invasive and relatively cheap technique. Cell growth, cell activity, changes in cell composition and shape or in cell location are examples of processes which can be detected with microelectrode-cell impedance sensors [6-9]. Among Impedance Spectroscopy (IS) techniques, Electrical Cell-substrate Impedance Spectroscopy (ECIS) [7.8], based on two-electrode setups, allows the measure of cell-culture impedance and the definition of the biological nature (material, internal activity, motility and size) of a kind of cell and its relationship with the environment [11]. One of the main drawbacks of ECIS technique is the need of efficient models to decode the electrical performance of the full system composed by the electrodes, medium and cells. Several works have been developped in this field. In [8], magnitude and phase impedance are deduced from electric field equation solution at the cell-electrode interface, giving a three parameter based model. h, the cell-electrode distance, R_b, barrier resistance and r_{cell}, cell radius. In [9,10], finite element simulation (FEM) are executed for solving electrical field considering the whole structure. This method gives one parameter model (R_{gap}) for describing the gap or cell-electrode region resistance. In both, the derived model considers the cell confluent phase [7] or a fixed area covered by cells [9]. The latest was extended in [10] to several cell sizes, allowing to define the cell-electrode covered area as the main model parameter.

Manuscript received March 26, 2011. This work was supported in part by the Spanish founded Project: Auto-calibración y auto-test en circuitos analógicos, mixtos y de radio frecuencia: Andalusian Government project P0-TIC-5386, co-financed with FEDER program.

[1] A. Yúfera is with the Seville Microelectronics Institute (IMSE-CNM), Seville Uni.. Av. Americo Vespucio, sn, 41092, Seville. Spain. Phone: +34954466666. yufera@imse-cnm.csic.es.

[2] P. Daza is with the Dpt. of Cell Biology, Biology Faculty. Seville Uni. Av. Reina Mercedes, sn, 41012, Seville. Spain. pdaza@us.es.

[3] D. Cañete is with the Dpt. of Electronic Technology, ETSII, Seville Uni.. Av. Reina Mercedes, sn, 41012, Seville. Spain. dani@zariweyo.es.

This work considers a modification of model in [9], to incorporate the cell-microelectrode area overlap [10]. Impedance sensor sensitivity curves based on the cell size and density will be presented and applied to measure the growth-tax in cell-cultures and to describe cell toxicity experiments. Section II resumes the electrode solution model useful for cell-electrode characterization. The process to extract useful cell-microelectrode models is included at section III, illustrating the simulations on a simplified system for cell size detection. Section IV relies on real time cell culture monitoring and the application of the proposed model to dosimetry experiments. Conclusions will be highlighted at section V.

II. ELECTRODE-ELECTROLYTE MODEL

The impedance of electrodes in ionic liquids has been rather extensively investigated. An excellent review can be found at [6]. The main componets describing the electrical performance of an electrode metal inside a solution are four: the double layer capacitance, C_I, the current flowing through the electrified interface will encounter a resistance R_{ct} caused by the electron transfer at the electrode surface and Warburg impedance Z_W due to limited mass diffusion from the electrode surface to the solution. The electron transfer resistance R_{ct} is in series with the mass diffusion limited impedance Z_W. As the current spreads out to the bulk solution, the electrode has a solution conductivity determined by series resistance, represented as spreading resistance R_S in the equivalent circuit. These four parameters depend on technology, medium and geometry.

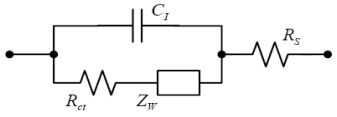

Figure 1. Circuit for the electrode-solution interface. C_I is the double layer capacitance, Faradic impedance includes Z_w, the Warburg impedance and R_{ct}, the charge-transfer resistance. R_s is the spreading resistance.

III. CELL-ELECTRODE MODEL

Figure 2 illustrates a two-electrode impedance sensor useful for ECIS technique: e_1 is the sensing electrode and e_2 the reference one. Electrodes can be manufactured in CMOS process with metal layers [9] or using post-processing steps [13]. The cell location and size on e_1 top must be detected.

The model in Fig. 3 considers the sensing surface of e_1 could be total or partially filled by cells. For the two-electrode sensor in Fig. 2, e_1 is the sensing area A, and $Z(\omega)$ the impedance by unit area of the empty electrode (without cells on top). When e_1 is partially covered by cells in a surface A_c, $Z(\omega)/(A-A_c)$ is the electrode impedance associated to non-covered area by cells, and $Z(\omega)/A_c$ is the impedance of the covered area. R_{gap} models the current flowing laterally through the electrode-cell interface, which depends on the electrode-cell distance at the

interface (in the range of 15-150nm). For an empty electrode, the impedance model Z(ω) is represented by the circuit in Fig. 1. It has been considered for e_2 the model in Fig 3a, not covered by cells. The e_2 electrode is commonly large and ground connected, being its resistance small enough to be rejected. Figure 4 represents the impedance magnitude, Z_c, for the sensor system in Fig. 2, considering that e_1 could be either empty, partially or totally covered by cells. The parameter *ff*, called *fill factor*, is zero for A_c=0 (e_1 electrode empty), and one for A_c=A (e_1 electrode full). It is defined Z_c (*ff*=0)=Z_{nc} as the impedance magnitude of the sensor without cells.

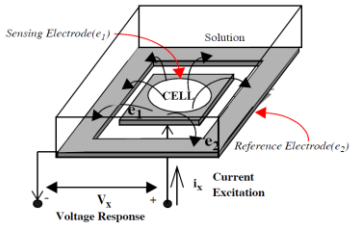

Figure 2. Two electrodes for ECIS: e_1 (sensing) and e_2 (reference). AC current i_x is injected between e_1-e_2, and voltage response V_x is measured.

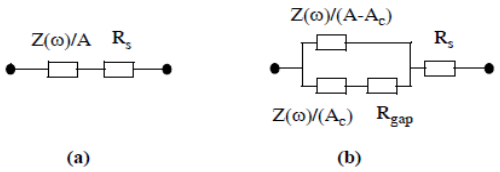

Figure 3. Proposed model for the an electrode-solution-cell model with area A, uncovered with cells (a) and covered and area A_c (b).

The relative changes at impedance magnitude, defined as,

$$r = \frac{Z}{Z_{nc}} \quad (1)$$

informs more accurate from these variations, being r the change of impedance magnitude for the two-electrode with cells (Z_c) with respect to the system without them (Z_{nc}). The graphics of *r* versus frequency is plotted in Fig. 5, for a cell-to-electrode coverage ff from 0.1 to 0.9 in steps of 0.1, using a R_{gap}=90 kΩ. The size of the electrode is 32x32 μm^2 [9,10]. It can be identified again the frequency range where the sensitivity to cells is high at 100kHz, represented by r increments. For a given frequency, each value of the normalized impedance r can be linked with its ff, being possible the cell detection and estimation of the covered area A_c. Even more, A_c can be intrepreted as consequence than two or more cells, allowing cell count for a given cell size.

From Fig. 5, it can be deduced that models of electrode-cell electrical performance can be used to derive the overlapping area in cell-electrode systems, useful for biological studies. It can be observed how the curve fits well with the frequency range, placing the maximum r value around 100kHz, as predicts the FEM simulations [9,10]. A value of R_{gap}=90kΩ was selected for this curve, representing a maximum value of the r curve with ff=0.69, which represents the ratio (A_c/A), for a cell size of 30μm diameter represented at figure obtained using FEM simulations [10]. Impedance sensor curves at figures 4 and 5 were obtained using SpectreHDL [14] mixed-mode simulator, with Analog Hardware Description Language (AHDL) for circuits in Fig. 3. A potential advantage of using AHDL models is the possibility to include non-linear performance of circuit elements, in our case the frequency square root function at the Warburg impedance.

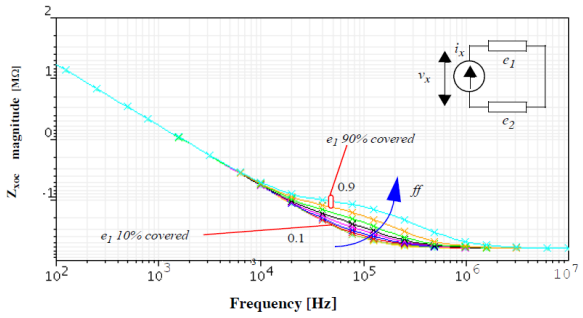

Figure 4. Impedance evolution when fill factor increases 32 x 32 μm^2.

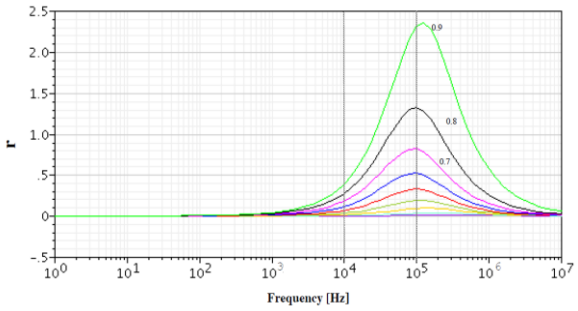

Figure 5. Normalized impedance r versus frequency. Curves correspond to a fill factor in the range of 0.1 (near empty) to 0.9 (near full).

IV. Cell Culture Applications

A: Electrode Model

The proposed model based in Fig 3 has three main parameters: the electrode area (A), the fill-factor (ff), and the resistance of the gap region (R_{gap}). Technology data were included and simulation results obtained to model a commercial electrode: 8W10E, from Applied Biophysics [12]. It is composed by eight wells; each one contains ten circular gold microelectrodes, with 250μm diameter. Ten sensing electrodes, in paralell, were used for e_1 and only one common reference electrode, much larger than sensing ones. Figure 6 represents the normalized impedance r expected for these electrodes, for R_{gap}=22kΩ, if fill factor changes from electrodes without cell on top (ff=0.1) to near those fully covered (ff=0.9). Values of R_{gap} can be used to match the models to observed performance. In Fig. 7, R_{gap} values were changed for ff=0.9, observing large r changes. Finally, it was also modifyed the electrode area for R_{gap}=22kΩ and ff=0.9, showing the results at Fig. 8. It can be observed that optimal working frequency is near the proposed by the electrode factory (around 4kHz), and that electrode area covered by cells can be approximated by using the ff parameters. The performance curves obtained can be used to fit experimental results to proposed model and find relevant biometric characteristics.

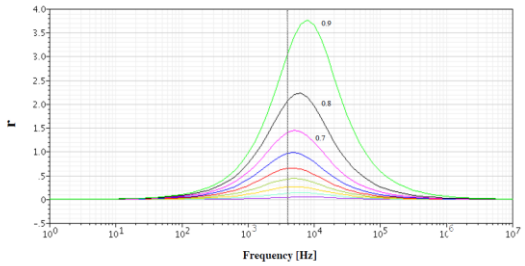

Figure 6. Normalized impedance r vs frequency, for ff ∈ [0.1,0.9] and R_{gap} = 22kΩ, using m 8W10E electrodes.

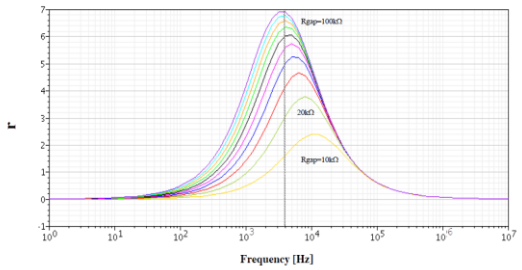

Figure 7. Normalized impedance r vs frequency, for R_{gap} ∈ [10kΩ,100kΩ] in steps of 10kΩ, for ff=0.9, using 8W10E electrodes.

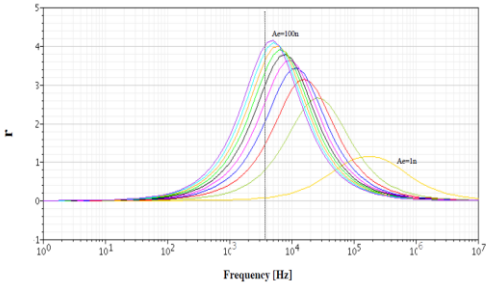

Figure 8. Normalized impedance r vs frequency, for R_{gap}=22kΩ and ff=0.9, for differents electrode areas (1n-100n). 49n ($49.10^{-9}m^2$) corresponds to a circular electrode with a 250μm diameter.

B: Cell growth

Figure 9a shows the growthing curve measure by us during seven days using 8W10E sensors with a similar setup in [8]. AA8 cells from chinese hamster were seeded initially, in an approximated number of 5000. The impedance range is 1220Ω (380Ω–1600Ω), for 4kHz frequency. Considering an initial cell number of 5000 very low, we take the initial impedance as due to no-cell impedance value (Z_{nc}). At t=6000 min, the medium was changed, and the confluent phase was achieved at t = 8500 min approximately. The maximum experimental value given from eq. (1) is around r = 3.1, as illustrates Fig. 9b. If we consider that the electrodes are aproximatelly fully covered by cells for ff=0.9, the value of R_{gap} that better fits is 22kΩ. System response corresponds to r-values illustrated in Fig. 6. From these curves, are obtained the fill factor at different times. Table I summarized the relative normalized impedance values r versus time. Using Fig. 6 for the sensor response, fill factor is calculated at every instant. For a well area of 0.8 cm^2, the maximum number of cells goes from $0.8x10^6$ to $1.6x10^6$. Number of cells, n_{cell}, in Table I, is obtained from $0.8x10^6$ expected final value of cell. A value of Z_{nc}=380Ω for *r* calculus at eq. (1) was considered.

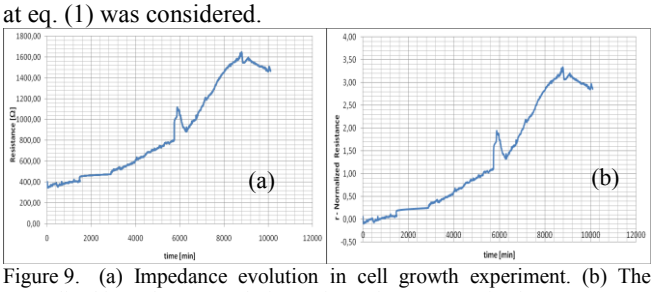

Figure 9. (a) Impedance evolution in cell growth experiment. (b) The normalised impedance r evolution estimated. Frequency is 4kHz.

Table I: Number of cells (n_{cell}) obtained from impedance Z_c measure in Fig. 6, and using the r curves proposed for 8W10E sensors.

t (min)	r	ff	n_{cell}
0	0	-	5000
500	0.024	0.020	18000
1000	0.050	0.050	44000
1500	0.072	0.070	63000
2000	n.a.	n.a.	n.a.
2500	n.a.	n.a.	n.a.
3000	0.374	0.362	322000
3500	0.437	0.395	351000
4000	0.615	0.475	422000
4500	0.777	0.530	471000
5000	0.903	0.581	516000
5500	1.033	0.602	535000
6000	1.074	0.620	551000
6500	1.507	0.710	631000
7000	1,970	0.775	689000
7500	2,353	0.810	720000
8000	2,837	0.860	764000
8500	3.113	0.890	791000
9000	3.134	0.900	800000
9500	3.010	0.875	778000
10000	2,857	0.864	768000

C: Dosimetry

Experiments for characterizing the influence of some drugs to cell growth were also done. The objective is to proof that proposed model allows counting cell number at different dosis. It was considered the AA8 cell line and as drug, six different doses of MG132 for growth inhibition (from 0.2μM to 50μM). After 72 hours normal cell growth, the medium was changed and the drug added at different doses: 0.2, 0.5, 1, 5, 10 and 50μM for wells 3 to 8 respectively. Well 2 is the control.

Experimental impedances obtained for the 8 wells are represented at Fig. 10, for 4kHz frequency. At the end of the experiment can be observed that impedance decreases as drug dosis increases. Control (W2) is full of cells with the maximum impedance, while maximum dosis (W8) has the lowest resistance, at the botton. The black line (W1) represents the electrode-solution impedance. After the medium change (t=4000min), it is observed in W1 a decreasing impedance below the initial baseline level (400Ω) that we cannot explain. Final impedance values at 8000min, Z_c, were considered at Table II. From Z_{nc} and Z_c, r values are calculated at thirth column. Using curves for r in Fig. 6, ff estimated values from proposed model are obtained. The cell number at the end of the experiment was also count, and is shown at the last column for each well. Considering ff_{max}=0.9 for a number of cell of $8.06x10^5$ experimentally measured, the expected values for ff are calculated.

The same data are summarized at Table III for 2, 4 and 10kHz

frequencies respectively. The better agreement it is obtained at 4kHz in fill factor (ff). It is observed that the impedance baseline, Z_{nc}, for r calculus decreases with frequency due probably to electrode impedance dependence. For medium resistance (W1) and high drug concentrations wells (W6-W8), the resistance measured is below to Z_{nc}, so eq. (1) can not be applied for r calculus.

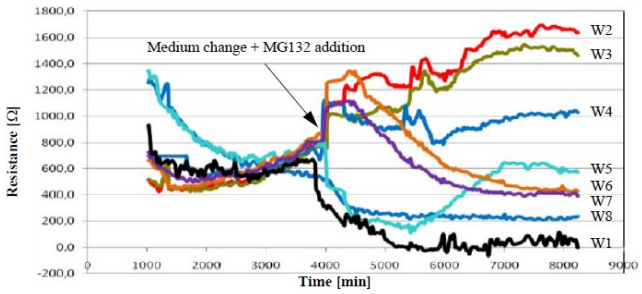

Figure 10. Impedance measure in dosimetry at 8 wells for 4 kHz frequency. W1: Medium. W2: Control. W3: 0.2 μM. W4: 0.5 μM. W5: 1 μM. W6: 5 μM. W7: 10 μM and W8: 50 μM.

Table II: Experimental values for relative impedance (r) and fill-factor (ff). Z_{nc} = 400 Ω. Frequency = 4 kHz.

Well	Z_c t=8000min	r Z_c ,$\mathbf{Z_{nc}}$	ff estimated	ff expected	n_{cell} measured
1	259.2	-	-	-	Medium
2	1631.7	3.1	0.90	0.900	$8.06x10^5$
3	1454.7	2.6	0.85	0.690	$6.13x10^5$
4	1030.6	1.5	0.72	0.610	$5.41x10^5$
5	625.8	0.5	0.44	0.410	$3.60x10^5$
6	417.4	0.05	0.037	0.036	$3.20x10^4$
7	406.8	0.015	0.016	0.024	$2.10x10^4$
8	99.6	< 0	-	0.005	$4.00x10^3$

Table III: Experimental values for relative impedance (r) and fill-factor (ff) at different frequencies. Z_{nc} = 480Ω, 400Ω, and 315Ω for 2, 4 and 10 kHz working frequencies respectively.

	r from Z_c and Z_{nc}			ff Estimated from model			ff expected
Well	2kHz	4kHz	10kHz	2kHz	4kHz	10kHz	
1	-	-	-	-	-	-	Medium
2	2.43	3.1	3.76	0.98	0.90	0.90	0.900
3	2.18	2.6	3.24	0.94	0.85	0.88	0.690
4	1.17	1.5	2.21	0.82	0.72	0.82	0.610
5	0.21	0.5	0.84	0.32	0.44	0.44	0.410
6	-	0.05	-	-	0.037	-	0.036
7	-	0.015	-	-	0.016	-	0.024
8	-	-	-	-	-	-	0.005

V. Discussion and Conclusions

This work described the application of an area parametrized model for cell-electrode system to measure and identify cells in cell culture experiments. A practical circuit for electrode-solution-cell simulation was employed, using an AHDL description for commercial electrodes, obtaining a good matching. Optimal measurement frequency was identified near 4kHz. It was proposed the cell growth evolution study based on 8W10E electrode models. Curves obtained experimentally, allows the real time growth monitoring by fitting the R_{gap} parameter. An estimation of the number of cells was obtained by using sensor curves calculated from electrical model proposed. Dosimetry experiments reproduce similar conditions than cell growth, but in this case, it is added a growth inhibitor at different dosis. It was observed a decreasing impedance, below the baseline expected (Z_{nc}) that we can not explain. However, for the control and small drug dosis, impedance curves are perfectly aligned. It was fitted a proposed model with R_{gap}=22kΩ to explain experiemental data. Deviations from data are over 10-20% in fill factor, more accurate for 4kHz.

The deviations in fill factors measured are large, being necessary to analize the influence of some error sources to increase the system performance. First, Signal-to-Noise Ratio (SNR) should be increased at the setup. Second, proposed model has the advantage that need only one parameter (R_{gap}), versus other reported model using three parameters [8]. One parameter model makes easy to fit experimental data, but also introduce inaccuracy. The possibility to add more parameters to the model should be considered at the future.

Acknowledgements

We would like to thanks to Citoquimica Ultraestructural Group (BIO132) of Cell Biology Department, Seville University, for its experimental help to develop the cell culture experiments.

References

[1] Grimnes, S. and Martinsen, O., "Bio-impedance and Bioelectricity Basics," *Second edition. Academic Press, Elsevier*. 2008.

[2] R. D. Beach et al., "Towards a Miniature In Vivo Telemetry Monitoring System Dynamically Configurable as a Potentiostat or Galvanostat for Two- and Three- Electrode Biosensors," *IEEE Transaction on Instrumentation and Measurement*, vol 54, nº1, pp:61-72. 2005.

[3] A.Yúfera et al., "A Tissue Impedance Measurement Chip for Myocardial Ischemia Detection," *IEEE Transaction on Circuits and Systems: Part I*. vol.52, nº 12 pp: 2620-2628. 2005.

[4] S. Radke et al., "Design and Fabrication of a Microimpedance Biosensor for Bacterial Detection" *IEEE Sensor J*. vol 4,nº 4,434-440.2004.

[5] A. Yúfera et al., "A Method for Bioimpedance Measure With Four- and Two-Electrode Sensor Systems," *30th Annual International IEEE EMBS Conference*, pp: 2318-2321. 2008.

[6] D. A. Borkholder. Cell-Based Biosensors Using Microelectrodes. PhD Thesis, Stanford University. 1998.

[7] I. Giaever and C. R. Keese, "Use of Electric Fields to Monitor the Dynamical Aspect of Cell Behaviour in Tissue Cultures," *IEEE Trans. on Biomedical Engineering*, vol. BME-33, nº 2, pp: 242-247. 1986.

[8] I. Giaever and C. R. Keese, "Micromotion of mammalian cells measured electrically," *Proc. Nail. Acad. Sci. USA. Cell Biology*, vol. 88, pp: 7896-7900, Sep. 1991.

[9] X. Huang et al., "Simulation of Microelectrode Impedance Changes Due to Cell Growth," *IEEE Sensors J*., vol.4, nº 5, pp: 576-583. 2004.

[10] A. Olmo et al., "Computer Simulation of Microelectrode Based Bio-Impedance Measurements With COMSOL," *BIODEVICES 2010*. pp: 178-182. Valencia (Spain), 20-23, Jan. 2010.

[11] P. Wang and Q. Liu, editors. Cell-Based Biosensors: Principles and Applications, *Artech House Series*. 2010.

[12] Applied Biophysics. Http://www.biophysics.com/.

[13] A. Manickam, A. Chevalier, M. McDermott, A. D. Ellington, and A. Hassibi, "A CMOS Electrochemical Impedance Spectroscopy (EIS) Biosensor Array," *IEEE Transactions on Biomedical Circuits and Systems*, vol 4, nº 6. pp: 379-390. 2010.

[14] SpectreHDL Reference Manual, Cadence Design Systems Inc.

[15] A. Yúfera and A. Rueda, "A Real-Time Cell Culture Monitoring CMOS System Based on Bio-impedance Measurements," Kluwer Academic Pub: Analog Integrated Circuits and Signal Processing. 2011. (accepted)